Proceedings of 2018 IEEE
International Conference on Mechatronics and Automation
August 5 - 8, Changchun, China

Control for balance of Legged-Wheel Hybrid Robot(LWHR) by regulating ground reaction force with kinematic coupling

SeungJae Yoo[1] and YongHwan Oh[2]
Department of HCI & Robotics, KIST School
Korea University of Science and Technology(UST)
Daejeon, 305-350, Korea
{*seungjae, oyh*}*@kist.re.kr*

***Abstract*— This paper is concerned with a novel control method for a legged-wheel hybrid robot(LWHR). We first derive a contact map from ground reaction forces(GRF) to linear and angular forces on center of mass(CoM). To resolve the lack of rank condition of the contact map due to an existance of reciprocal axis, each of the GRF at the contact points are regulated by a reformed linear invertible contact map while remained forces on the CoM are handled by the kinematic coupling on the conservation of momentum. It would be worthly to remark that there are no singular cases because the reformed contact map has full rank condition kinematically as long as the constraint of each wheels is active. As a result, by this method, we can fully manage all forces on the CoM by which the balance control is accomplished. Finally, we demonstrate the effectiveness of the methods through some simulation results.**

***Index Terms*— Multi-contact balancing, Legged-wheel robot, Whole-body control, Contact map, Momentum conservation control**

I. Introduction

Studies on interaction with robots and humans has been brought attention to robotics community. Since there are demands for assistant robots to alleviate physical works, a number of mobile devices have been developed. Although many mobile devices are equipped with wheels due to simplicity and efficiency of its mechanical design [1], a number of legged robots have been challenged to cover those issues such as ASIMO [2], ATLAS [3], and ATRIAS [4]. The legged mobile system is considered that it can be relatively robust than the wheeled mobile system because it can adjust to terrain [5]. In this sense, the legged-wheel hybrid robot(LWHR) consisting of the characteristics of both legged and wheeled mobile robots could have not only flexibility but also energy efficiency on the arbitrary terrain. Thus, there have been a number of studies on wheel-legged mobile systems with more than two legs such as Rover [6], [7], and AWR [8]. However there are few studies on wheel based bipedal robots [5], [9] which are even far from general shape of bipedal models.

A number of studies dealing with biped robots have employed inverted pendulm as their reduced models [10], [11]. This is because such an inverted pendulum model allows to alleviate complexity of multi-dynamic models. These intuition could be strong because the control strategies on the reduced model can be map back to full dynamics [12].

Several methods for balance control of wheeled mobile and biped systems have been developed such as ZMP [13], CP [14] in which linear motion of a Center of Mass(CoM) is regulated. Although these models have been very beneficial for the sense of balance, there are no cosiderations on rotational dynamics which also plays a significant role [12]. In fact, linear and angular motion of the CoM in two-wheeled mobile system cannot be fully regulated because there is a reciprocal axis between contact points of each wheels which will be discussed in the control section.

In this paper, we do not design a reduced model and focus on the linear and angular forces on the CoM generated by Ground Reaction Force(GRF). In other words, the balance control is accomplished by regulating the GRF of the each wheels which are obtained by a contact map to desired linear and angular forces at the CoM. Due to the reciprocal axis, the contact map is reformed to invertible linear map with an output constraint. This novel method has advantages that there are no singular cases as long as the constraint of each contacts is maintained.

For regulating robot's kinematic pose without the GRF, the control of free-floating body is considered which have been addressed in the several researchs of space robot area [15], [16]. Due to dynamic coupling with robot's free-floating body and joint motions, the task space kinematic velocities of the body can be expressed in joint space which is called Generalized Jacobian [16]. By this method, the kinematic pose can be regulated on the conservation of momentum.

II. Modeling LWHR

The LWHR is equipped with 2 legs with n number of joints and a floating body by which the system has $(2n+6)$ Degrees of Freedom(DoF). A velocity of body coordinates is defined as

$$\boldsymbol{\xi}_B \equiv \begin{bmatrix} \dot{\boldsymbol{p}}_B \\ \boldsymbol{\omega}_B \\ \dot{\boldsymbol{q}} \end{bmatrix} \in \mathbb{R}^{2n+6} \tag{1}$$

where $\dot{\boldsymbol{p}}_B, \boldsymbol{\omega}_B \in \mathbb{R}^3$ are linear and angular velocities of body and $\boldsymbol{q} = \begin{bmatrix} q_{11} & \cdots & q_{1n} & q_{21} & \cdots & q_{2n} \end{bmatrix}^T \in \mathbb{R}^{2n}$ are each

978-1-5386-6075-1/18/$31.00 ©2018 IEEE

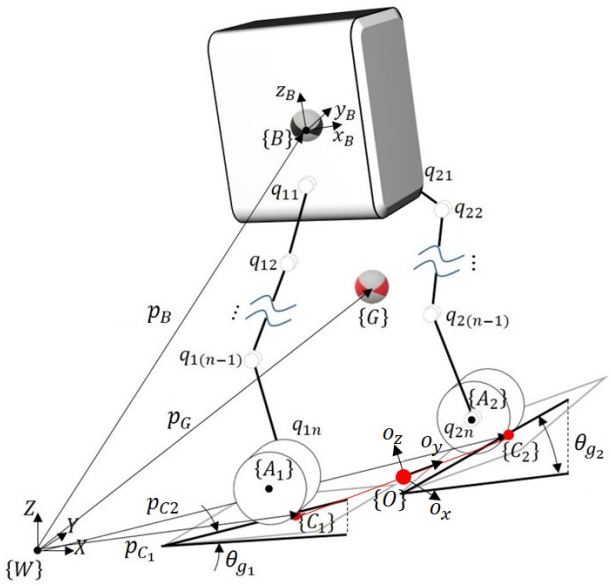

Fig. 1. Legged-Wheel Hybrid Robot(LWHR): Each legs are equipped with n joints and a wheel at n^{th} joint. The contact points $\{C_1\},\{C_2\}$ are considered as end effectors of this system.

joint angles. The each wheels are equipped with the in^{th} joint where $i=1$ means the right leg and $i=2$ means the left leg. The body's($\{B\}$) linear and anguler postions, velocities from the world frame($\{W\}$) are assumed to be directly estimated.

A. Positions and Velocities

Positions and orientations of ij^{th} joints(l_{ij}) from $\{W\}$ are

$$\begin{cases} \boldsymbol{p}_{l_{ij}} = \boldsymbol{p}_B + \boldsymbol{R}_B \boldsymbol{p}^B_{Bl_{ij}} \\ \boldsymbol{R}_{l_{ij}} = \boldsymbol{R}_B \boldsymbol{R}^B_{Bl_{ij}} \end{cases} \tag{2}$$

where $i=1,2,\ j=1,\cdots,n$ and $\boldsymbol{R}\in SO(3)$. The notation $(\bullet)^B_{Bl_{ij}}$ means from $\{B\}$ to l_{ij} regard to $\{B\}$ frame($\{W\}$ is not noted). Linear and anguler velocities of ij^{th} joints are

$$\boldsymbol{v}_{l_{ij}} \equiv \begin{bmatrix} \dot{\boldsymbol{p}}_{l_{ij}} \\ \boldsymbol{\omega}_{l_{ij}} \end{bmatrix} = \begin{bmatrix} \boldsymbol{J}_{l_{ij},v} \\ \boldsymbol{J}_{l_{ij},\omega} \end{bmatrix} \boldsymbol{\xi}_B = \boldsymbol{J}_{l_{ij}} \boldsymbol{\xi}_B \tag{3}$$

where $\boldsymbol{J}_{l_{ij},v}, \boldsymbol{J}_{l_{ij},\omega} \in \mathbb{R}^{3\times(2n+6)}$ denote linear and anguler Jacobians from $\{W\}$ and. The Jacobian of CoM forms as a following equation.

$$\dot{\boldsymbol{p}}_G = \boldsymbol{J}_{G,v}\boldsymbol{\xi}_B \equiv \begin{bmatrix} \boldsymbol{B}_G^T & \hat{\boldsymbol{J}}_{BG,v} \end{bmatrix} \begin{bmatrix} \boldsymbol{v}_B \\ \dot{\boldsymbol{q}} \end{bmatrix} \tag{4}$$

where $\boldsymbol{B}_G \in \mathbb{R}^{6\times3}$, $\hat{\boldsymbol{J}}_{BG,v} \in \mathbb{R}^{3\times2n}$ and $\boldsymbol{v}_B = \begin{bmatrix} \dot{\boldsymbol{p}}_B^T & \boldsymbol{\omega}_B^T \end{bmatrix}$.

B. Contact points

To figure out contact points $\{C_i\}$, θ_{A_i} and θ_{g_i} must be determined as shown in Fig. 2 because these are not related

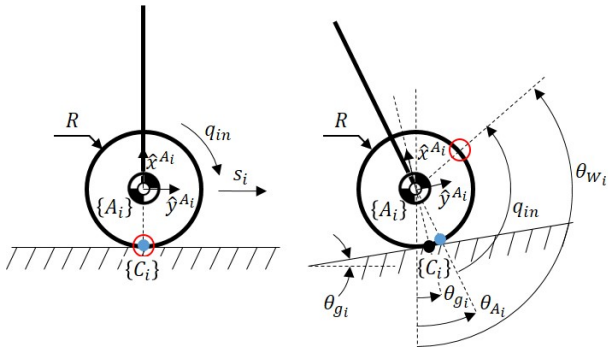

Fig. 2. The view of i^{th} wheel on $x^{A_i}-y^{A_i}$ plane: The red circle is fixed on the wheel and the blue disk is a intersection point between the wheel and extended line of the last leg. It shows that a tatal rotation angle of the wheel is $\theta_{W_i} = q_{in} + \theta_{A_i}$ while an actual angle of the wheel joint is q_{in}.

with last joint angles q_{1n}, q_{2n}. Let the slope angle θ_{g_i} be known and θ_{A_i} can be calculated from

$$\boldsymbol{R}_{A_i}\boldsymbol{R}(z,\theta_{g_i}) = \boldsymbol{R}_{l_{in}}\boldsymbol{R}(z,\theta_{A_i}) \tag{5}$$

where $\boldsymbol{R}(z,\theta_{A_i})$, $\boldsymbol{R}(z,\theta_{g_i})$ are rotation matrixs with θ_{A_i}, θ_{g_i} by z-axis. There is a slippery error at the each of contact points that

$$\dot{\boldsymbol{p}}_C \equiv \begin{bmatrix} \dot{\boldsymbol{p}}_{C_1} \\ \dot{\boldsymbol{p}}_{C_2} \end{bmatrix} = \begin{bmatrix} \boldsymbol{J}_{C_1,v} \\ \boldsymbol{J}_{C_2,v} \end{bmatrix} \boldsymbol{\xi}_B = \boldsymbol{J}_C \boldsymbol{\xi}_B \tag{6}$$

where $\boldsymbol{J}_{C_i,v} \in \mathbb{R}^{3\times(2n+6)}$ denote the each of contact Jacobians. With non-slip condition, $\dot{\boldsymbol{p}}_C = 0$ must be satisfied.

C. Equation of motion for LWHR

The equation of motion of the LWHR with the contact constraints forms as

$$\begin{cases} \boldsymbol{M}(\boldsymbol{q})\dot{\boldsymbol{\xi}}_B + \boldsymbol{n}(\boldsymbol{\xi}_B,\boldsymbol{q}) = \boldsymbol{\Gamma} + \boldsymbol{J}_C^T \boldsymbol{f}_C \\ \boldsymbol{J}_C \boldsymbol{\xi}_B = 0 \end{cases} \tag{7}$$

and more specifically

$$\begin{bmatrix} \boldsymbol{M}_{bb} & \boldsymbol{M}_{bq} \\ \boldsymbol{M}_{qb} & \boldsymbol{M}_{qq} \end{bmatrix} \begin{bmatrix} \dot{\boldsymbol{v}}_B \\ \ddot{\boldsymbol{q}} \end{bmatrix} + \begin{bmatrix} \boldsymbol{n}_b \\ \boldsymbol{n}_q \end{bmatrix} = \begin{bmatrix} 0 \\ \boldsymbol{\tau} \end{bmatrix} + \boldsymbol{J}_C^T \boldsymbol{f}_C \tag{8}$$

$$\boldsymbol{J}_C = \begin{bmatrix} \boldsymbol{E}_3 & -[\boldsymbol{p}_{BC_1}] & \hat{\boldsymbol{J}}_{BC_1,v} \\ \boldsymbol{E}_3 & -[\boldsymbol{p}_{BC_2}] & \hat{\boldsymbol{J}}_{BC_2,v} \end{bmatrix}, \quad \boldsymbol{f}_C \equiv \begin{bmatrix} \boldsymbol{f}_{C_1} \\ \boldsymbol{f}_{C_2} \end{bmatrix} \tag{9}$$

where $\boldsymbol{E}_3 \in \mathbb{R}^3$, $\hat{\boldsymbol{J}}_{BC_i,v} \in \mathbb{R}^{3\times2n}$ denote an identity matrix and a Jacobian of joint coordinates from body to each contact points. The $[\boldsymbol{p}] \in \mathbb{R}^{3\times3}$ represents a skew-symmetric matrix of a vector $\boldsymbol{p} \in \mathbb{R}^3$. The $\boldsymbol{\tau} \in \mathbb{R}^{2n}$, $\boldsymbol{f}_{C_i} \in \mathbb{R}^3$ are a joint input torque vector and forces at the each contact point. A $\{G\}$ frame coordinates is necessary to figure out the contact map from the contact forces to CoM which can be earned by a following map from $\boldsymbol{\xi}_G$ to $\boldsymbol{\xi}_B$.

$$\boldsymbol{\xi}_B = \underbrace{\begin{bmatrix} \boldsymbol{E}_3 & -[\boldsymbol{p}_{GB}] & -\hat{\boldsymbol{J}}_{BG,v} \\ 0_3 & \boldsymbol{E}_3 & 0 \\ 0 & 0 & \boldsymbol{E}_{2n} \end{bmatrix}}_{\equiv \boldsymbol{Q}_{BG}^T} \underbrace{\begin{bmatrix} \dot{\boldsymbol{p}}_G \\ \boldsymbol{\omega}_B \\ \dot{\boldsymbol{q}} \end{bmatrix}}_{\equiv \boldsymbol{\xi}_G} \tag{10}$$

where $\boldsymbol{Q}_{BG} \in \mathbb{R}^{(2n+6)\times(2n+6)}$ denotes a coodinate transform matrix from $\{G\}$ to $\{B\}$. The contact map is derived by (7), (10) as

$$\begin{aligned}\boldsymbol{J}_C\boldsymbol{\xi}_B &= \boldsymbol{J}_C\boldsymbol{Q}_{BG}^T\boldsymbol{\xi}_G \\ &= \underbrace{\begin{bmatrix} \boldsymbol{E}_3 & -[\boldsymbol{p}_{GC_1}] \\ \boldsymbol{E}_3 & -[\boldsymbol{p}_{GC_2}] \end{bmatrix}}_{\equiv \boldsymbol{G}_C^T} \underbrace{\begin{bmatrix} \hat{\boldsymbol{J}}_{GC_1,v} \\ \hat{\boldsymbol{J}}_{GC_2,v} \end{bmatrix}}_{\equiv \hat{\boldsymbol{J}}_{GC}} \boldsymbol{\xi}_G \end{aligned} \tag{11}$$

where $\boldsymbol{G}_C \in \mathbb{R}^{6\times 6}$ is the contact map to the CoM.

III. Control

A. Balance control

For the balance control, the linear and angular force at the CoM must be figured out. Define $\boldsymbol{\lambda}_G \equiv \begin{bmatrix} \boldsymbol{f}_G^T & \boldsymbol{\mu}_G^T \end{bmatrix}^T$ in which $\boldsymbol{f}_G \equiv \begin{bmatrix} f_{G,x} & f_{G,y} & f_{G,z} \end{bmatrix}^T \in \mathbb{R}^3$ is a linear force at the CoM and $\boldsymbol{\mu}_G \equiv \begin{bmatrix} \mu_{G,x} & \mu_{G,y} & \mu_{G,z} \end{bmatrix}^T \in \mathbb{R}^3$ is an angular force at the CoM. From the principle of virtual work, the contact map between the CoM and the contact points is derived by following equation.

$$\begin{aligned}&\boldsymbol{\tau}^T\dot{\boldsymbol{q}} - \boldsymbol{f}_C^T\dot{\boldsymbol{p}}_C - \boldsymbol{\lambda}_G^T\boldsymbol{v}_G = 0 \\ &\Rightarrow (\boldsymbol{\tau}^T - \boldsymbol{f}_C^T\hat{\boldsymbol{J}}_{GC})\dot{\boldsymbol{q}} - (\boldsymbol{f}_C^T\boldsymbol{G}_C^T + \boldsymbol{\lambda}_G^T)\boldsymbol{v}_G = 0\end{aligned} \tag{12}$$

where $\boldsymbol{v}_G = \begin{bmatrix} \dot{\boldsymbol{p}}_G^T & \boldsymbol{\omega}_G^T \end{bmatrix}$. The contact map from $\boldsymbol{f}_C$ to $\boldsymbol{\lambda}_G$ is derived by (11) as

$$\begin{cases} \underbrace{\begin{bmatrix} \boldsymbol{f}_G \\ \boldsymbol{\mu}_G \end{bmatrix}}_{\boldsymbol{\lambda}_G} = \underbrace{\begin{bmatrix} \boldsymbol{E}_3 & \boldsymbol{E}_3 \\ [\boldsymbol{p}_1] & [\boldsymbol{p}_2] \end{bmatrix}}_{\boldsymbol{G}_C} \underbrace{\begin{bmatrix} \boldsymbol{f}_1 \\ \boldsymbol{f}_2 \end{bmatrix}}_{\boldsymbol{f}_r} \\ \boldsymbol{\tau} = \hat{\boldsymbol{J}}_{GC}^T\boldsymbol{f}_C \end{cases} \tag{13}$$

where $\boldsymbol{p}_i = \boldsymbol{p}_{GC_i}$ and $\boldsymbol{f}_r$ is the GRFs with $\boldsymbol{f}_i = -\boldsymbol{f}_{C_i}$. However the $\boldsymbol{f}_i = \begin{bmatrix} f_{i,x} & f_{i,y} & f_{i,z} \end{bmatrix}^T$ satisfing the arbitray $\boldsymbol{\lambda}_G$ is not exist generally due to $rank(\boldsymbol{G}_C) = 5$. What a condition makes the lack of rank can be figured out by decomposing the contact map $\boldsymbol{G}_C$ as

$$\boldsymbol{\lambda}_G = \underbrace{\begin{bmatrix} \boldsymbol{E}_3 & 0_3 \\ [\boldsymbol{p}_{GO}] & \boldsymbol{E}_3 \end{bmatrix}}_{\boldsymbol{L}} \underbrace{\begin{bmatrix} \boldsymbol{E}_3 & \boldsymbol{E}_3 \\ -[\delta\boldsymbol{p}] & [\delta\boldsymbol{p}] \end{bmatrix}}_{\boldsymbol{O}_C} \boldsymbol{f}_r \tag{14}$$

where $\boldsymbol{p}_{GO} = \frac{1}{2}(\boldsymbol{p}_1 + \boldsymbol{p}_2)$ and $\delta\boldsymbol{p} = \frac{1}{2}(\boldsymbol{p}_2 - \boldsymbol{p}_1)$ as shown in Fig. 1. The (14) can be expressed in $\{O\}$ frame as

$$\underbrace{(\boldsymbol{L}\boldsymbol{R}_{O,6})^{-1}\boldsymbol{\lambda}_G}_{\boldsymbol{\lambda}_O^O} = \boldsymbol{O}_C^O\boldsymbol{f}_r^O \tag{15}$$

$$\boldsymbol{R}_{O,6} = \begin{bmatrix} \boldsymbol{R}_O & 0_3 \\ 0_3 & \boldsymbol{R}_O \end{bmatrix}, \begin{cases} \boldsymbol{R}_O = \begin{bmatrix} \boldsymbol{o}_x & \boldsymbol{o}_y & \boldsymbol{o}_z \end{bmatrix} \\ \boldsymbol{o}_x = \boldsymbol{o}_y \times \begin{bmatrix} 0 & 0 & 1 \end{bmatrix}^T \\ \boldsymbol{o}_y = \frac{\delta\boldsymbol{p}}{|\delta\boldsymbol{p}|} \\ \boldsymbol{o}_z = \boldsymbol{o}_x \times \boldsymbol{o}_y \end{cases} \tag{16}$$

Here, it can be easily identified that the lack of rank occur at 5^{th} row of $\boldsymbol{O}_C^O$ becasue its elements are all zero. It means that $\mu_{O,y}^O$ is not controllable by the contact forces. Therefore, the reference command $\boldsymbol{\lambda}_G$ must be designed to satisfy $\mu_{O,y}^O = 0$, in other words, we have an output constraint that

$$\mu_{G,y}^O = p_{GO,z}^O f_{G,x}^O - p_{GO,x}^O f_{G,z}^O \tag{17}$$

where $\boldsymbol{p}_{GO}^O = \boldsymbol{R}_O^T\boldsymbol{p}_{GO}$ and $\boldsymbol{f}_G^O = \boldsymbol{R}_O^T\boldsymbol{f}_G$. To satisfy it, we design the $\boldsymbol{\lambda}_G$ as an following "set and re-set" method.

$$\begin{aligned}&\text{set: } \boldsymbol{\lambda}_G = \begin{bmatrix} 0 \\ 0 \\ f_{G,z} \\ \mu_{G,x} \\ \mu_{G,y} \\ \mu_{G,z} \end{bmatrix} \Rightarrow \boldsymbol{\lambda}_G^O = \boldsymbol{R}_{O,6}^T\boldsymbol{\lambda}_G = \begin{bmatrix} 0 \\ f_{G,y}^O \\ f_{G,z}^O \\ \mu_{G,x}^O \\ \mu_{G,y}^O \\ \mu_{G,z}^O \end{bmatrix} \\ &\text{re-set: } \boldsymbol{\lambda}_G^O = \begin{bmatrix} \frac{\mu_{G,y}^O + p_{GO,x}^O f_{G,z}^O}{p_{GO,z}^O} \\ f_{G,y}^O \\ f_{G,z}^O \\ \mu_{G,x}^O \\ \mu_{G,y}^O \\ \mu_{G,z}^O \end{bmatrix} \Rightarrow \boldsymbol{\lambda}_G = \boldsymbol{R}_{O,6}\boldsymbol{\lambda}_G^O \end{aligned} \tag{18}$$

where $f_{G,x}, f_{G,y}$ is determined to satisfy the equation (17) and these forces are handled indirectly that will be discussed in the next subsection. As noted in (18), we decide the rotational motion of LWHR for the balance control in the sense of that the system would not fall down with specified $\boldsymbol{\mu}_G$. Also, an invertible linear map from $\boldsymbol{f}_r$ to $\boldsymbol{\lambda}_G$ can be derived by left muliplying equation (14) with $\boldsymbol{L}^{-1}$ as following that

$$\underbrace{\begin{bmatrix} \boldsymbol{f}_O \\ \boldsymbol{\mu}_O \end{bmatrix}}_{\boldsymbol{\lambda}_O} = \begin{bmatrix} \boldsymbol{f}_1 + \boldsymbol{f}_2 \\ [\delta\boldsymbol{p}](\boldsymbol{f}_2 - \boldsymbol{f}_1) \end{bmatrix} = \underbrace{\begin{bmatrix} \boldsymbol{f}_1 + \boldsymbol{f}_2 \\ \delta\boldsymbol{p} \times \delta\boldsymbol{f} \end{bmatrix}}_{=\boldsymbol{O}_C\boldsymbol{f}_r} \tag{19}$$

where $\delta\boldsymbol{f} = \boldsymbol{f}_2 - \boldsymbol{f}_1$. The equation (19) shows that $\boldsymbol{\mu}_O \perp \delta\boldsymbol{p}$ and $\boldsymbol{\mu}_O \perp \delta\boldsymbol{f}$ by which the unit vector $\hat{\boldsymbol{f}} = \frac{\delta\boldsymbol{f}}{|\delta\boldsymbol{f}|}$ can be expressed as the rotation of $\hat{\boldsymbol{p}} = \frac{\delta\boldsymbol{p}}{|\delta\boldsymbol{p}|}$ by $\hat{\boldsymbol{\mu}} = \frac{\boldsymbol{\mu}_O}{|\boldsymbol{\mu}_O|}$ with θ_o as shown in Fig. 3. The invertible linear map from $\boldsymbol{f}_r$ to $\boldsymbol{\lambda}_G$ is earned by following equation.

$$\begin{aligned}\boldsymbol{\lambda}_O &= \begin{bmatrix} \boldsymbol{f}_O \\ |\delta\boldsymbol{p}||\delta\boldsymbol{f}|\sin\theta_o\hat{\boldsymbol{\mu}} \end{bmatrix} = \begin{bmatrix} \boldsymbol{f}_O \\ |\delta\boldsymbol{p}||\delta\boldsymbol{f}|\sin\theta_o\boldsymbol{R}_{\theta_o}\hat{\boldsymbol{f}} \end{bmatrix} \\ &= \underbrace{\begin{bmatrix} \boldsymbol{E}_3 & 0_3 \\ 0_3 & |\delta\boldsymbol{p}|\sin\theta_o\boldsymbol{R}_{\theta_o} \end{bmatrix}}_{\equiv\boldsymbol{L}_p} \underbrace{\begin{bmatrix} \boldsymbol{E}_3 & \boldsymbol{E}_3 \\ -\boldsymbol{E}_3 & \boldsymbol{E}_3 \end{bmatrix}}_{\equiv\boldsymbol{L}_f} \boldsymbol{f}_r \end{aligned} \tag{20}$$

where $\boldsymbol{R}_{\theta_o} = \boldsymbol{R}(\hat{\boldsymbol{p}}, 90^\circ)\boldsymbol{R}(\hat{\boldsymbol{\mu}}, 90^\circ - \theta_o)$ represents a rotation matrix from $\hat{\boldsymbol{\mu}}$ to $\hat{\boldsymbol{f}}$. With specified θ_o, therefore, the contact force $\boldsymbol{f}_r$ can be calculated by a following equation.

$$\boldsymbol{f}_r = \boldsymbol{L}_f^{-1}\boldsymbol{L}_p^{-1}\boldsymbol{L}^{-1}\boldsymbol{\lambda}_G \tag{21}$$

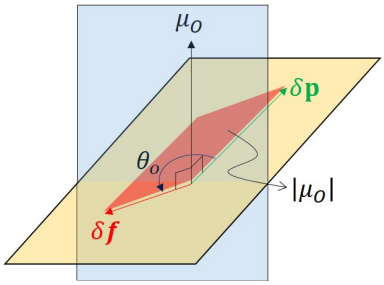

Fig. 3. The relation $\boldsymbol{\mu}_O = \delta \boldsymbol{p} \times \delta \boldsymbol{f}$ where $\delta \boldsymbol{p} = \boldsymbol{p}_2 - \boldsymbol{p}_1$, $\delta \boldsymbol{f} = \boldsymbol{f}_2 - \boldsymbol{f}_1$, and $\boldsymbol{\lambda}_O = \boldsymbol{L}^{-1}\boldsymbol{\lambda}_G$.

Here, we choose $\theta_o = 90^\circ$ to minimize $|\delta \boldsymbol{f}|$. As a result, $\boldsymbol{f}_{C_1}, \boldsymbol{f}_{C_2}$ are obtained from desired arbitrary command $\boldsymbol{\lambda}_G$ on the specified θ_o with the output constraint $\mu^O_{O,y} = 0$. As a result, the joint input torque is

$$\boldsymbol{\tau}_G = \hat{\boldsymbol{J}}^T_{GC} \boldsymbol{f}_C \tag{22}$$

B. Indirect control $f_{G,x}, f_{G,y}$

So far the contact forces $\boldsymbol{f}_{C_1}$, $\boldsymbol{f}_{C_2}$ satisfying the desired $\boldsymbol{f}_G, \tau_G$ are figured out except $f_{G,x}, f_{G,y}$. The x axis linear force $f_{G,x}$ is determined by the contact map. Therefore, its desired value should be handled kinematically. The only controllable position variables are $p_{1,x}, p_{2,x}$ because positions of y and z direction are not controllable by the non-slip condition. The equation to figure out desired x direction positions $p^*_{1,x}, p^*_{2,x}$ for following the desired x direction force at CoM $f^*_{G,x}$ is

$$\underbrace{\begin{bmatrix} f^*_{G,x} \\ \delta^*_x \\ \mu_{G,y} \\ \mu_{G,z} \end{bmatrix}}_{\boldsymbol{b}} = \underbrace{\begin{bmatrix} 1 & 1 & 0 & 0 \\ 0 & 0 & -1 & 1 \\ p_{1,z} & p_{2,z} & -f_{1,z} & -f_{2,z} \\ -p_{1,y} & -p_{2,y} & f_{1,y} & f_{2,y} \end{bmatrix}}_{\boldsymbol{A}} \underbrace{\begin{bmatrix} f^*_{1,x} \\ f^*_{2,x} \\ p^*_{1,x} \\ p^*_{2,x} \end{bmatrix}}_{\boldsymbol{x}^*} \tag{23}$$

where $\delta^*_x = p^*_{2,x} - p^*_{1,x}$ is a desired x-direction distance between contact points and the $\boldsymbol{A} \in \mathbb{R}^{4\times4}$ always satisfy $rank(\boldsymbol{A}) = 4$ kinematically. Therefore, $p^*_{1,x}, p^*_{2,x}$ can be earned by $\boldsymbol{x}^* = \boldsymbol{A}^{-1}\boldsymbol{b}$. The desired contact forces $f^*_{1,x}$, $f^*_{2,x}$ satisfying $f_{G,x} = f^*_{G,x}$ is generated at $p_{1,x} = p^*_{1,x}$, $p_{2,x} = p^*_{2,x}$. By simliar way, the $p^*_{1,y}, p^*_{2,y}$ satisfying $f^*_{G,y}$ can be earned.

The second task is the position control from $\boldsymbol{p}_i$ to $\boldsymbol{p}^*_i$ without the contact forces. Due to dynamic coupling between robot's free-floating body and joint motions, the lagrange D'lambert equation of robot without external forces is

$$\frac{d}{dt}\left(\frac{\partial K_{sys}}{\partial \boldsymbol{v}_B}\right) - \nabla_{\boldsymbol{p}_B} K_{sys} = 0 \tag{24}$$

where $K_{sys} = \frac{1}{2}\boldsymbol{\xi}^T_B \boldsymbol{M}(\boldsymbol{q})\boldsymbol{\xi}_B$ is kinetic energy of the robot and $\nabla_{\boldsymbol{p}_B} K_{sys} = 0$ because the K_{sys} is not a function of $\boldsymbol{p}_B$. By integrating (24), we get the momentum equation that

$$\boldsymbol{M}_{bb}\boldsymbol{v}_B + \boldsymbol{M}_{bq}\dot{\boldsymbol{q}} = const. \tag{25}$$

For now, let us consider this term equal to zero by which the relative velocity between the contact points and the CoM is obtained by joint coordinates as

$$\begin{aligned} \dot{\boldsymbol{p}}_C &= \boldsymbol{B}^T_C \boldsymbol{v}_B + \hat{\boldsymbol{J}}_{BC}\dot{\boldsymbol{q}} \\ &= \underbrace{(\hat{\boldsymbol{J}}_{BC} - \boldsymbol{B}^T_C \boldsymbol{M}^{-1}_{bb}\boldsymbol{M}_{bq})}_{\equiv \boldsymbol{J}_{C,g}}\dot{\boldsymbol{q}} \end{aligned} \tag{26}$$

where $\boldsymbol{B}^T_C \in \mathbb{R}^{6\times6}$, $\hat{\boldsymbol{J}}_{BC} \in \mathbb{R}^{6\times2n}$ denotes block matrices of the Jacobian $\boldsymbol{J}_C = \begin{bmatrix} \boldsymbol{B}^T_C & \hat{\boldsymbol{J}}_{BC} \end{bmatrix}$. The $\boldsymbol{J}_{C,g} \in \mathbb{R}^{6\times2n}$ is called a Generalized Jacobian [15] by which any joint torques transformed are always satisfing conservation of system's momentum [16]. Finally a total joint input $\boldsymbol{\tau}$ is

$$\boldsymbol{\tau} = \boldsymbol{\tau}_G + \boldsymbol{J}^T_{C,g}\boldsymbol{f}_{\boldsymbol{p}} \tag{27}$$

where $\boldsymbol{f}_{\boldsymbol{p}} = \begin{bmatrix} \boldsymbol{f}^T_{\boldsymbol{p}_1} & \boldsymbol{f}^T_{\boldsymbol{p}_2} \end{bmatrix}$, $\boldsymbol{f}_{\boldsymbol{p}_i} \in \mathbb{R}^3$ are forces to manage each of the contact positions $\boldsymbol{p}_i$. It is worthwhile to remark that $\boldsymbol{J}^T_{C,g}\boldsymbol{f}_{\boldsymbol{p}}$ do not affect $\boldsymbol{\lambda}_G$ generated by $\boldsymbol{\tau}_G$. This can be easily verified by substituting (27) for $\boldsymbol{\tau}$ in (12).

$$\begin{aligned} &(\boldsymbol{\tau}^T - \boldsymbol{f}^T_C\hat{\boldsymbol{J}}_{GC})\dot{\boldsymbol{q}} - (\boldsymbol{f}^T_C\boldsymbol{G}^T_C + \boldsymbol{\lambda}^T_G)\boldsymbol{v}_G = 0 \\ &\Rightarrow \boldsymbol{f}^T_{\boldsymbol{p}}\underbrace{\boldsymbol{J}_{C,g}\dot{\boldsymbol{q}}}_{\dot{\boldsymbol{p}}_C = 0} - (\boldsymbol{f}^T_C\boldsymbol{G}^T_C + \boldsymbol{\lambda}^T_G)\boldsymbol{v}_G = 0 \end{aligned} \tag{28}$$

C. Desired forces and torques

The desired force and torques $\boldsymbol{\lambda}_G$ must be defined to specify the desired contact forces $\boldsymbol{f}_{C_1}, \boldsymbol{f}_{C_2}$. The control target is that the $f_{G,z}$ is decided for maintaining the height with gravity compensation and τ_G is decided for regulating the orientation of the body. For the height control, the $f_{G,z}$ is

$$f_{G,z} = k_{P,z}(p_{G,z,d} - p_{G,z}) + k_{D,z}(\dot{p}_{G,z,d} - \dot{p}_{G,z}) + m_{tot}g \tag{29}$$

where $k_{P,z}, k_{D,z}$ are proportional and derivative gains for height control and $p_{G,z,d}, \dot{p}_{G,z,d}$ are desired z axis position and velocity of the CoM. Before design the desired angular force $\boldsymbol{\mu}_G$, the difference between the desired and present orientation $\delta\boldsymbol{R} \in \mathbb{R}^{3\times3}$ should be defined as

$$\delta\boldsymbol{R} = \tilde{\boldsymbol{R}}^T_B\boldsymbol{R}_d \tag{30}$$

where $\tilde{\boldsymbol{R}}_B$, $\boldsymbol{R}_d$ denote a present and desired orientation regard to local coordinates. The local coordinates is decided by the equation $\tilde{\boldsymbol{R}}_B \equiv \boldsymbol{R}_B\boldsymbol{R}(z,\psi)$ where $\boldsymbol{R}_B$ represents a present orientation regard to the world frame and the ψ is an angle between the world and local frame. Here, the error of orientation expressed in ZYX eular angles $\boldsymbol{\phi} = \begin{bmatrix} \phi_x & \phi_y & \phi_z \end{bmatrix}^T$ can be extracted from $\delta\boldsymbol{R}$ and the desired τ_G is

$$\boldsymbol{\mu}_G = \boldsymbol{K}_{P,o}\boldsymbol{\phi} - \boldsymbol{K}_{D,o}\tilde{\boldsymbol{\omega}}_B \tag{31}$$

where $\boldsymbol{K}_{P,o}, \boldsymbol{K}_{D,o} \in \mathbb{R}^{3\times3}$ are proportional and derivative gains and $\tilde{\omega}_B = \boldsymbol{R}(z,\psi)\omega_B$ is an angular velocity of the body regard to the local coordinates. For the indirect control, the $\boldsymbol{f}_{\boldsymbol{p}_i}$ are

$$\boldsymbol{f}_{\boldsymbol{p}_i} = \boldsymbol{K}_{P,i}(\tilde{\boldsymbol{p}}^*_i - \tilde{\boldsymbol{p}}_i) - \boldsymbol{K}_{D,i}\tilde{\boldsymbol{v}}_i \tag{32}$$

where $\tilde{\boldsymbol{p}}_i = \boldsymbol{R}(z,\psi)\boldsymbol{p}_i$ and $\boldsymbol{K}_{P,i}, \boldsymbol{K}_{D,i} \in \mathbb{R}^{3\times3}$ represent proportional and derivative gains.

IV. Simulation

A. Kinematics of the LWHR system

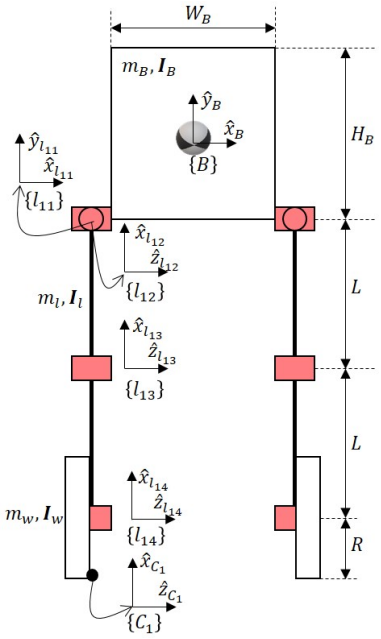

Fig. 4. Each of frames and notations of properties: $H_B = 0.4m$, $W_B = 0.6m$, $L = 0.5m$, $R = 0.15m$, $m_B = 15kg$, $m_l = 1.5kg$, $m_w = 1.5kg$, $I_B = diag(0.65, 0.5, 0.25)(kg \cdot m^2)$, $I_l = diag(0.000938, 0.0121, 0.0121)(kg \cdot m^2)$, $I_w = diag(0.0004, 0.0004, 0.03375)(kg \cdot m^2)$

TABLE I

DH PARAMETERS

i^{th} Leg	θ	d	a	α
$\{B\}$ to l_{i1}	$\pi/2$	$-H_B/2$	$sgn(i)W_B/2$	$\pi/2$
l_{i1} to l_{i2}	$q_{i1}+\pi/2$	0	0	$\pi/2$
l_{i2} to l_{i3}	q_{i2}	0	$-L$	0
l_{i3} to l_{i4}	q_{i3}	0	$-L$	0
l_{i4} to $\{C_i\}$	$\theta_{A_i} - \theta_{g_i}$	0	$-R$	0

The simulation model has 4 joints at each legs $(n = 4)$. DH parameters and frames are noted in TABLE I and Fig. 4 where $sgn(1) = -1, sgn(2) = 1$ and the slope angles $\theta_{g_1}, \theta_{g_2}$ are given by feedforward. Therefore, the LWHR is fully actuated by regulating the 6 contact forces and the 2 relative positions of contact points. The control gains are decided as

$$\begin{aligned} K_{P,z} &= 100, \quad K_{D,z} = 50 \\ \boldsymbol{K}_{P,o} &= diag(30,30,30), \quad \boldsymbol{K}_{D,o} = diag(10,10,10) \\ \boldsymbol{K}_{P,i} &= diag(500,0,0), \quad \boldsymbol{K}_{D,i} = diag(30,0,0) \end{aligned} \tag{33}$$

B. Result of Simulation

The desired angle commands of orientation are all zero and the desired x direction force command is $f^*_{G,x} = k_{D,x}(\dot{p}_{G,x,d} - \dot{p}_{G,x}) - \ddot{p}_{G,x}$ where $\dot{p}_{G,x,d}, \dot{p}_{G,x}$ are desired and present x direction velocities of CoM and $\ddot{p}_{G,x}$ is earned recursively(we set $\dot{p}_{G,x,d} = 5m/s, k_{D,x} = 10$). On the result of the simualtion, the balance control is accomplished well although there are 3 slopes and impacts as shown in Fig. 5 which shows robustness on terrain. In this paper, the balance target is to regulate the rotational motion of the body in which the pitching and yawing errors ϕ_y, ϕ_z are fairly well restored through the obstacles while the rolling error ϕ_x needs more time for converging to zero as shown in Fig. 7. It makes sense because the x direction linear force at the contact points cannot handle the rolling motion while y direction linear force at the contact points are not handled in this simulation due to lack of joint DoF.

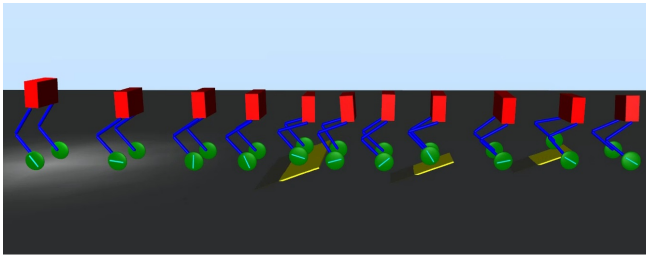

Fig. 5. A simulation with 3 obstacles (MuJoCo): There are 3 panels located at $2m$ intervals with 20° slope and $0.5m$ length. The first one affect both wheels simultaneously and the others affect each wheels seperately. The average velocity of the CoM is $2.1m/s$ on the simulation.

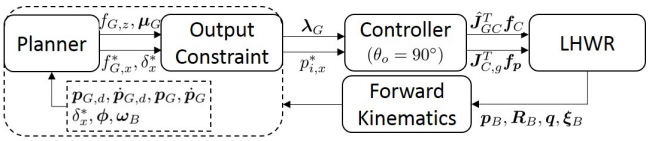

Fig. 6. Block diagram of the controller on the simulation

As discussed in the control section, the x-axis linear force is determined by the contact map while we manage it indirectly. This desired linear force regulated by the relative positions of each wheels is displayed in Fig 8. The error of relative positions of each contact points are fairly small by which the force is tracked despite several obstacles. It shows that a linear velocity of progress direction can be handled without consideration of the balance.

V. Conclusion

In this paper, we design legged-wheel hybrid robot(LWHR) with two of a n DoF leg. On the specific construction, each legs have 4 joints($n = 4$) by which total system has 14 DoF. The balance control is accomplished by regulating the rotational motion of the body. The contact map is decomposed and transformed to the invertible linear map by specifying the output constraints. The remained linear forces are handled indirectly by the relative motion of wheels from the CoM because those are determined to satisfy the contact map on given kinematic pose. The linear map is designed to get the relative positions of

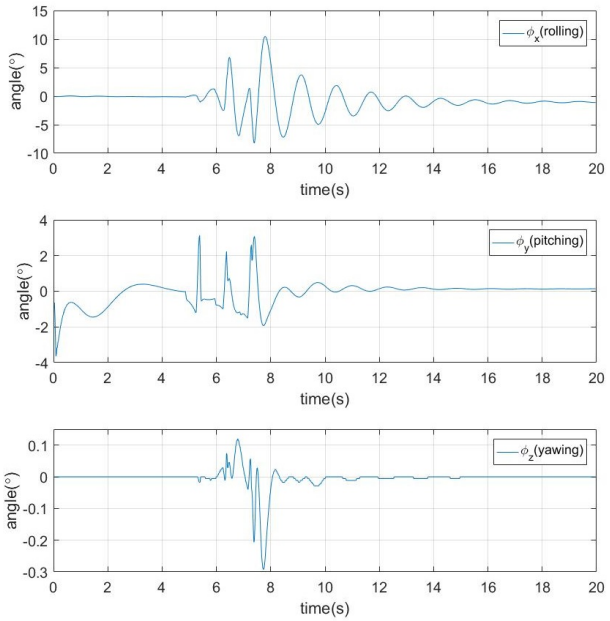

Fig. 7. The errors of orientation (ZYX euler angle): It shows the rolling, pitching, and yawing errors of orientation depending on time. It can be a indicator of how the balance control is accomplished because the contact forces are regulated by this errors.

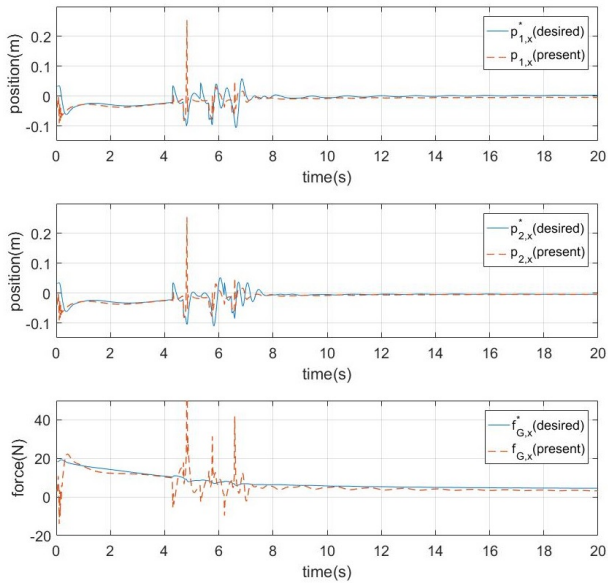

Fig. 8. The relative postions of the contact points(above 2) and the force of the CoM on x axis: Blue line shows that desired relative positions and a force of x-direction. Red line shows that acture relative positions and a force of x-direction. This result shows that $f_{G,x}$ can be handled indirectly by regulating $p_{1,x}$ and $p_{2,x}$.

each wheels generating the desired remained linear forces. The Generalized Jacobian is derived from the momentum equation by which the relative motion of wheel can be specified with the conservation of the robot's momentum.

The novel contribution of this paper is that there are no singular cases for the balance control with the non-slip condition. As long as the constraints of each wheels are active, this method can always figure out the contact forces not to fall down from arbitrary disturbances. In other words, it contains robustness through some obstacles as shown in simulation section. Also, the reason of properties for the force based control, it shows compliant motion which is shown in the simulation results where the variation of robot's height is fairly small through several obstacles.

REFERENCES

[1] Munzir Zafar, Henrik I. Christensen, "Whole Body Control of a Wheeled Inverted Pendulum Humanoid", IEEE/International Conference on Humanoid Robots(Humanoids), 2016

[2] Yoshiaki Sakagami, Ryujin Watanabe, et al. "The intelligent ASIMO: System overview and integration", IEEE/International Conference on Intelligent Robots and Systems(IROS), 2002

[3] Wyatt Newman, Zheng-Hao Chong, et al. "Autonomous Valve Turning with an Atlas Humanoid Robot", IEEE/International Conference on Humanoid Robots(Humanoids), 2014

[4] Christian Hubicki, Jesse Grimes, et al. ATRIAS: Design and validation of atether-free 3D-capable spring-mass bipedal robot, International Journal of Robotics Research(IJRR), 2016

[5] Kenji Hashimoto, Hun-ok Lim, Atsuo Takanishi, et al. "Realization by Biped Leg-wheeled Robot of Biped Walking and Wheel-driven Locomotion", IEEE/International Conference on Robotics and Automation(ICRA), 2005

[6] Christophe Grand, Faiz Ben Amar, et al. Motion kinematics analysis of wheeled-legged rover over 3D surface with posture adaptation, Mechanism and Machine Theory(MMT), 2010

[7] Christophe Grand, Faiz Ben Amar, et al. Stability and Traction Optimization of a Reconfigurable Wheel-Legged Robot, International Journal of Robotics Research(IJRR), 2004

[8] Qiushi Fu, Venkat Krovi, "Ariticulated Wheeled Robots: Exploiting Reconfigurability and Redundacy", Dynamic Systems and Control Conference(DSCC), 2008

[9] Osamu Matsumoto, Shuuji Kajita, et al. "Dynamic Trajectory Control of Passing Over Stairs by a Biped Type Leg-wheeled Robot with Nominal Reference of Static Gait", IEEE/International Conference on Intelligent Robots and Systems(IROS), 1998

[10] Shuuji Kajita, Fumio Kanehiro, et al. "The 3D Linear Inverted Pendulum Mode: A simple modeling for a biped walking pattern generation", IEEE/International Conference on Intelligent Robots and Systems(IROS), 2001

[11] Sung-Hee Lee, Ambarish Goswami, "Ground reaction force control at each foot: A momentum-based humanoid balance controller for non-level and non-stationary ground", IEEE/International Conference on Intelligent Robots and Systems(IROS), 2010

[12] Sung-Hee Lee, Ambarish Goswami, "Reaction Mass Pendulum (RMP): An explicit model for centroidal angular momentum of humanoid robots", IEEE/International Conference on Robotics and Automation(ICRA), 2007

[13] Tomomich Sugihara, Toshihiko Nakamura, et al. "Realtime Humanoid Motion Generation through ZMP Manipulation based on Inverted Pendulum Control", IEEE/International Conference on Robotics and Automation(ICRA), 2002

[14] Johannes Englsberger, Christian Ott, et al. "Bipedal walking control based on Capture Point dynmics", IEEE/International Conference on Intelligent Robots and Systems(IROS), 2011

[15] Kazuya Yoshida, Dragomir N. Nechev, A General Formulation of Under-Actuated Manipulator Systems, IEEE/International Conference on Intelligent Robots and Systems(IROS), 1998

[16] Luis Sentis, Oussama Khatib, "Control of Free-Floating Humanoid Robots Through Task Prioritization", IEEE/International Conference on Robotics and Automation(ICRA), 2005